JOURNAL OF GUIDANCE, CONTROL, AND DYNAMICS
Vol. 32, No. 1, January–February 2009

Neighboring Optimum Feedback Control Law for Earth-Orbiting Formation-Flying Spacecraft

Jean-Francois Hamel* and Jean de Lafontaine†
Universite de Sherbrooke, Sherbrooke, Quebec J1K 2R1, Canada

DOI: 10.2514/1.32778

This paper develops a feedback control law that guarantees neighboring fuel-optimality of the reconfiguration of a formation of Earth-orbiting formation-flying spacecraft. It aims for the case in which a specific formation is to be achieved at a specific true anomaly. It guarantees neighboring fuel-optimality of such a reconfiguration maneuver, assuming that the formation evolves in the vicinity of an uncontrolled reference trajectory. It is in the semi-analytic form, as only one time-varying gain matrix needs to be computed before the maneuver. It allows a fuel consumption/formation accuracy tradeoff with the selection of only one scalar gain. Simulations compare the performance of this controller with the linear-quadratic regulator and the mean orbit elements controller in the context of a 1 km size formation reconfiguration. Simulations show that this neighboring optimum controller can perform the maneuver with better accuracy while spending as much or less propellant than the other controllers.

I. Introduction

FORMATION flying of spacecraft has, without any doubt, gained interest within the engineering and scientific community in recent years. This interest is most likely going to increase within the next years, mainly because of the numerous financial and operational advantages that formation flying can procure.

For example, missions using formation-flying spacecraft can potentially have a lower production cost due to economies of scale, in the case in which a single large and complex satellite is replaced by several mass-production smaller spacecraft. Also, using a constellation of spacecraft could decrease the cost of launch. Launching several smaller elements is potentially cheaper than launching a single big and heavy satellite, mainly because small satellites can be launched piggybacked on a larger spacecraft flight support equipment.

Moreover, spacecraft formation flying presents several operational advantages. The most important one is an increased robustness through failure recovery and graceful degradation. In missions using multiple spacecraft in formation, if a subsystem failure occurs in one of the spacecraft, another fully functional spacecraft could support the disabled spacecraft. The capabilities can be shared. For example, when a power, communication, or navigation system failure occurs in a spacecraft, it may be possible to use another spacecraft subsystem either by physically linking the spacecraft or by transmitting navigation information to the failed spacecraft. In the case of a separated spacecraft interferometer or a distributed antenna mission, the failure of one spacecraft would only cause a graceful degradation of the system, rather than compromising the whole mission. Thus, failure recovery and graceful degradation of the system decrease the risk of losing the mission. A second operational advantage is a mission restructuring capability. It is foreseeable to reconfigure the satellite formation on orbit to follow new mission requirements. Moreover, if the mission has multiple objectives, resources can be optimized by dispatching a certain group of spacecraft having special attributes to achieve one objective and then command another group of spacecraft to achieve another objective in parallel.

However, using a formation of spacecraft involves several challenges. The first one is an increase in the required level of autonomy. To minimize the resources needed for ground support, it is required to limit the command inputs to the system to high-level commands to the whole formation. The formation would then have to autonomously define lower-level commands to each of the spacecraft. The second challenge is the design of a fuel-optimal control system. Obviously, the formation reconfiguration and maintenance control algorithms have to minimize the fuel consumption of every spacecraft of the formation. However, fuel consumption also has to be balanced among the spacecraft to maximize the lifetime of the complete formation by ensuring that some spacecraft do not run out of fuel before the others.

The most studied formation-flying control architecture is, by far, the leader/follower type of architecture. Under this architecture, the relative motion control problem is reduced to the tracking of a desired trajectory defined as a position relative to a reference trajectory. The guidance system is typically responsible for defining a reference trajectory (that could be based on the states of one member of the formation or any virtual point in space) and a position and velocity relative to this reference trajectory for all of the members of the formation. In this context, several types of controllers using continuous and variable thrust (as opposed to impulsive thrust) have been developed for different assumptions and different relative motion models.

The simplest and most commonly used relative motion model is the Clohessy–Wiltshire–Hill (CWH) model [1]. It is linear and models unperturbed relative motion about a circular reference orbit. By using the CWH model of relative motion, conventional linear control can be applied to Earth-orbiting formation flying. The main advantage of linear control theory is that it is a well-known method, with measurable performance and robustness, assuming that the linearization conditions are valid. For example, the linear-quadratic regulator (LQR) uses a constant feedback gain matrix that minimizes the infinite-horizon state error and the quadratic actuator command. Ulybyshev [2] showed that a LQR can be used to maintain a planar formation on a circular orbit with good performance and robustness. Moreover, as will be shown later in this paper, the LQR can be applied to in-plane and out-of-plane maneuvers, even on an elliptical orbit. However, as is the case with many other control systems, increasing the controller gains reduces the response time of the controller but with an increased fuel cost. This controller is promising for long-term formation-keeping that only implies small maneuvers and small deviations from the reference state.

Presented at the AAS/AIAA Astrodynamics Specialists Conference, Mackinac Island, MI, 19–23 August 2007; received 12 June 2007; revision received 13 July 2008; accepted for publication 16 July 2008.

*Ph.D. Candidate, Department of Electrical Engineering, 2500 Boulevard Universite. Member AIAA.

†Professor, Department of Electrical Engineering, 2500 Boulevard Universite. Member AIAA.

Rahmani et al. [3] also developed an optimal reconfiguration maneuver of two spacecraft assuming CWH dynamics. The main conclusion of the work is that a balanced fuel-optimal maneuver of two spacecraft on an unperturbed circular orbit is achieved through equal and opposite acceleration of both spacecraft. However, those conclusions do not necessarily apply to elliptical and perturbed orbits. In fact, Inalhan et al. [4] demonstrated that assuming that the reference orbit is circular, even when the eccentricity is as small as 0.005, leads to a significant increase of fuel cost because the spacecraft fights the natural dynamics to keep the same relative trajectory as it would in a circular orbit.

On the other hand, the continuous mean orbit elements feedback control law, as developed by Schaub et al. [1,5] controls the current mean orbit elements vector of the spacecraft toward the desired mean orbit elements vector and is well suited for elliptical reference orbits. With this controller, it is possible to cooperate with the physics of orbital dynamics. Acting directly on the mean orbit elements allows the control of specific orbit elements at specific instants on the orbit to increase the fuel efficiency of the algorithm. For example, it is much more fuel-efficient to correct an inclination error at the equator than at the pole, whereas an error in the ascending node is easier to compensate near the poles. By carefully choosing the time-varying gain matrix of the controller, those effects can be accounted for.

A continuous Cartesian coordinates feedback control law has also been proposed by Schaub and Junkins [1]. If the desired trajectory is described as an inertial position and an inertial velocity, a control feedback law based on Cartesian coordinate errors can be used. Assuming that the relative orbits are J_2-invariant (no relative secular drift caused by J_2) and that the distance between the spacecraft is small, this simple feedback control law can make use of the nonlinear dynamics (such as J_2-perturbed dynamics) to compensate position and velocity errors. A similar control law, but adaptive to slowly varying spacecraft masses, has also developed by de Queiroz et al. [6].

The hybrid feedback law [1,7] uses desired states defined as a set of relative orbit element differences, and the tracking errors are Cartesian coordinate errors. The main advantage of this method is that the controller uses inputs that are easily measured (relative position and velocity in orbital frame) and the reference is defined as orbit elements, which is more conveniently expressed than rapidly evolving Cartesian coordinates.

However, none of these feedback controllers can ensure fuel-optimality for elliptical reference orbits. Moreover, their gains are difficult to tune and their convergence time is hard to predict, both reasons why these controllers are not particularly suited if a formation is to be attained only at a specific time or point of the orbit. The presence of several constraints in the problem, the nonlinearity of the dynamics, and the need for optimality make the optimal control theory a candidate of choice in this context. This theory can fuel-optimize or time-optimize any reconfiguration maneuver while considering perturbed and nonlinear dynamics. For circular reference orbits, an analytical solution can be obtained to get an analytical feedback law [8,9]. However, for reasonably complex and nonlinear dynamics, such as formation flying about an elliptical reference orbit, this method does require highly demanding numerical optimization iterations and does not guarantee convergence. Both of these characteristics preclude onboard implementation.

Semi-analytical solutions to the optimal reconfiguration problem can also be found in the rendezvous literature. Carter [8] solved the fuel-optimal rendezvous problem, assuming that the relative motion can be linearized. However, to be used in a feedback form, this solution requires constant online numerical resolution of integrals and matrix inversions during the maneuver. Some more recent work by Sharma et al. [10] analytically solved the optimal control problem for small formations on near-circular orbits and numerically built a near-optimal feedback controller around this trajectory. These solutions can be transposed to the formation-flying problem, but under the condition that each spacecraft is treated separately, which would cause the computational burden to increase with the number of spacecraft in the formation.

The neighboring optimal feedback controller presented in this paper uses an approach similar to the work of Sharma et al. [10], but is designed for the formation-flying problem. Similarly to the rendezvous solution, it is applicable to elliptical orbits and it does not require any online numerical optimization once the maneuver is started. However, it does not require a linearized model of motion and can make use of a model of reality that is as accurate as the user deems necessary. Moreover, the amount of up-front and in-flight computations are greatly reduced by simplifying assumptions. These assumptions hold as long as the formation evolves in the vicinity of a natural uncontrolled trajectory, which is desirable in a formation-flight context, but is rarely the case with the rendezvous problem. Finally, the proposed controller guarantees near-optimality for the whole formation with the same time-varying gain matrix. Hence, the complexity of the control system does not grow exponentially with the number of spacecraft in the formation.

Section II first lays the theory upon which the neighboring optimal controller is built. Then Sec. III applies the theory to the dynamics of formation flying. Finally, simulations that assess the performance of the feedback controller in comparison with other common controllers and the optimal open-loop solution are presented in Sec. IV.

II. Neighboring Optimum Feedback Law Theory

The general theory behind the neighboring optimum feedback control theory is summarized here for completeness. For a more detailed derivation of the theory, the reader is referred to the work of Bryson and Ho [11].

Optimal control theory provides a method for computing the control effort vector $\boldsymbol{u}(t)$ between the time t_0 and t_f that will minimize a cost function J of the form

$$J = \phi[\boldsymbol{x}(t_f)] + \int_{t_0}^{t_f} L[\boldsymbol{x}(t), \boldsymbol{u}(t), t]\mathrm{d}t \tag{1}$$

where $\boldsymbol{x}(t)$ are the states of the system, and the dynamics of the system are governed by

$$\dot{\boldsymbol{x}}(t) = f[\boldsymbol{x}(t), \boldsymbol{u}(t), t] \tag{2}$$

The optimization of J can be done with or without a fixed terminal time t_f and with or without terminal constraints $\psi[\boldsymbol{x}(t_f), t_f] = 0$ on the terminal states. In this section, we shall consider that the terminal time t_f is fixed. In a formation-flying scenario, this implies that the resulting controller is only applicable to maneuvers of a fixed duration or for which the formation is required at a specific point of the orbit.

The system dynamics can be adjoined to the cost function with a vector of Lagrange multipliers $\boldsymbol{\lambda}(t)$ and $\boldsymbol{\nu}(t)$. For convenience, we define the Hamiltonian H as

$$H = L(\boldsymbol{x}, \boldsymbol{u}, t) + \boldsymbol{\lambda}^T f(\boldsymbol{x}, \boldsymbol{u}, t) \tag{3}$$

so that the system dynamics and the cost function are adjoined in an augmented cost function $\bar{J}$:

$$\bar{J} = [\phi + \boldsymbol{\nu}^T \psi]_{t=t_f} + \int_{t_0}^{t_f} [L + \boldsymbol{\lambda}^T (f - \dot{\boldsymbol{x}})]\mathrm{d}t \tag{4}$$

If the value of the Lagrange multipliers is deliberately chosen to satisfy [11]

$$\dot{\boldsymbol{\lambda}}^T = -H_{\boldsymbol{x}} \tag{5}$$

where $H_{\boldsymbol{x}}$ denotes the Jacobian of H with respect to $\boldsymbol{x}$, with the boundary conditions

$$\boldsymbol{\lambda}^T(t_f) = \phi_{\boldsymbol{x}}(t_f) + \boldsymbol{\nu}^T \psi_{\boldsymbol{x}}(t_f) \tag{6}$$

Then the variation in $\bar{J}$ due to a variation of the control vector for fixed time t_0 and t_f reduces to

$$\delta \bar{J} = \boldsymbol{\lambda}^T(t_0)\delta \boldsymbol{x}(t_0) + \int_{t_0}^{t_f} H_{\boldsymbol{u}} \delta \boldsymbol{u} \mathrm{d}t \tag{7}$$

For an extremum, δJ must vanish for any arbitrary $\delta \boldsymbol{u}(t)$, which leads to the condition

$$H_{\boldsymbol{u}} = 0 \tag{8}$$

at any point in time between t and t_f. Therefore, the optimal value of the control vector $\boldsymbol{u}(t)$ and the resulting states $\boldsymbol{x}(t)$ are obtained by solving the system of differential equations:

$$\dot{\boldsymbol{x}} = f[\boldsymbol{x}(t), \boldsymbol{u}(t), t] \tag{9}$$

$$\dot{\boldsymbol{\lambda}} = -f_{\boldsymbol{x}}^T \boldsymbol{\lambda} - L_{\boldsymbol{x}} \tag{10}$$

with $\boldsymbol{u}(t)$ determined by

$$f_{\boldsymbol{u}}^T \boldsymbol{\lambda} + L_{\boldsymbol{u}} = 0 \tag{11}$$

with the boundary conditions

$$\boldsymbol{x}(t_0) = \boldsymbol{x}_0 \tag{12}$$

$$\boldsymbol{\lambda}^T(t_f) = \phi_{\boldsymbol{x}}(t_f) + \boldsymbol{\nu}^T \psi_{\boldsymbol{x}}(t_f) \tag{13}$$

and with the terminal conditions

$$\psi[\boldsymbol{x}(t_f), t_f] = 0 \tag{14}$$

Thus, solving this two-point boundary-value problem yields a control sequence $\boldsymbol{u}(t)$ that will bring the system from its initial states $\boldsymbol{x}_0$ to its final location at time t_f while minimizing the cost function J and complying with the terminal constraints ψ. If an analytical solution to the problem can be found, then the control law $\boldsymbol{u}(t)$ can become a feedback control law by replacing t_0 with t and $\boldsymbol{x}_0$ with $\boldsymbol{x}(t)$ in the solution. However, for reasonably complex problems, such as formation-flying dynamics about elliptical orbits, an analytical solution is difficult to obtain. The system needs to be numerically solved at each time step from t to t_f to obtain an optimal feedback control law. This is not suited for an onboard implementation. Therefore, alternative ways of simplifying the problem need to be found.

A less demanding solution (in terms of computational load) can be developed if the problem is linearized about the optimal path. The feedback control problem can be simplified if variations of the performance index about the optimal path are to be minimized. In this context, it is necessary to minimize second-order variations of the cost function because all first-order terms necessarily vanish about the optimal path.

Perturbations from the optimal path produced by a small initial state offset $\delta \boldsymbol{x}(t_0)$ and terminal conditions offset $\delta \psi$ are governed by the result of the linearization of the system described by Eqs. (9–14) around the optimal trajectory:

$$\delta \dot{\boldsymbol{x}} = f_{\boldsymbol{x}} \delta \boldsymbol{x} + f_{\boldsymbol{u}} \delta \boldsymbol{u} \tag{15}$$

$$\delta \dot{\boldsymbol{\lambda}} = -H_{\boldsymbol{xx}} \delta \boldsymbol{x} - f_{\boldsymbol{x}}^T \delta \boldsymbol{\lambda} - H_{\boldsymbol{xu}} \delta \boldsymbol{u} \tag{16}$$

$$0 = H_{\boldsymbol{ux}} \delta \boldsymbol{x} + f_{\boldsymbol{u}}^T \delta \boldsymbol{\lambda} + H_{\boldsymbol{uu}} \delta \boldsymbol{u} \tag{17}$$

$$\delta \boldsymbol{\lambda}(t_f) = \left[\left(\phi_{\boldsymbol{xx}} + \left(\boldsymbol{\nu}^T \psi_{\boldsymbol{x}} \right)_{\boldsymbol{x}} \right) \delta \boldsymbol{x} + \psi_{\boldsymbol{x}}^T d\boldsymbol{\nu} \right]_{t=t_f} \tag{18}$$

$$\delta \psi = [\psi_{\boldsymbol{x}} \delta \boldsymbol{x}]_{t=t_f} \tag{19}$$

where the notation $H_{\boldsymbol{xu}}$ denotes the Jacobian of H with respect to $\boldsymbol{x}$ and $\boldsymbol{u}$, such that

$$H_{\boldsymbol{xu}} = \frac{\partial}{\partial \boldsymbol{u}} (H_{\boldsymbol{x}})^T \tag{20}$$

In this context, we seek to minimize the second-order variation of the cost function J, as the first-order variations already vanish about the extremal path:

$$\delta^2 \bar{J} = \frac{1}{2} \left[\delta \boldsymbol{x}^T \left(\phi_{\boldsymbol{xx}} + \left(\boldsymbol{\nu}^T \psi_{\boldsymbol{x}} \right)_{\boldsymbol{x}} \right) \delta \boldsymbol{x} \right]_{t=t_f} \tag{21}$$

$$+ \frac{1}{2} \int_{t_0}^{t_f} [\delta \boldsymbol{x}^T \delta \boldsymbol{u}^T] \begin{bmatrix} H_{\boldsymbol{xx}} & H_{\boldsymbol{xu}} \\ H_{\boldsymbol{ux}} & H_{\boldsymbol{uu}} \end{bmatrix} \begin{bmatrix} \delta \boldsymbol{x} \\ \delta \boldsymbol{u} \end{bmatrix} \mathrm{d}t \tag{22}$$

Equations (15–19) instead form a linear two-point boundary-value problem, which is much easier to solve analytically than the complete optimal control problem. Assuming that $H_{\boldsymbol{uu}}$ is nonsingular (which is always the case if H is appropriately defined), the problem can be restated as

$$\delta \boldsymbol{u}(t) = -H_{\boldsymbol{uu}}^{-1} \left(H_{\boldsymbol{ux}} \delta \boldsymbol{x} + f_{\boldsymbol{u}}^T \delta \boldsymbol{\lambda} \right) \tag{23}$$

$$\delta \dot{\boldsymbol{x}} = A(t) \delta \boldsymbol{x} - B(t) \delta \boldsymbol{\lambda} \tag{24}$$

$$\delta \dot{\boldsymbol{\lambda}} = -C(t) \delta \boldsymbol{x} - A^T(t) \delta \boldsymbol{\lambda} \tag{25}$$

where

$$A = f_{\boldsymbol{x}} - f_{\boldsymbol{u}} H_{\boldsymbol{uu}}^{-1} H_{\boldsymbol{ux}} \tag{26}$$

$$B = f_{\boldsymbol{u}} H_{\boldsymbol{uu}}^{-1} f_{\boldsymbol{u}}^T \tag{27}$$

$$C = H_{\boldsymbol{xx}} - H_{\boldsymbol{xu}} H_{\boldsymbol{uu}}^{-1} H_{\boldsymbol{ux}} \tag{28}$$

This type of problem can be solved by the backward sweep method [11], and its solution takes the form

$$\delta \boldsymbol{\lambda}(t) = S(t) \delta \boldsymbol{x}(t) + R(t) \mathrm{d}\boldsymbol{\nu} \tag{29}$$

$$\delta \psi = R^T(t) \delta \boldsymbol{x}(t) + Q(t) \mathrm{d}\boldsymbol{\nu} \tag{30}$$

with the values of the S, R, and Q matrices governed by

$$\dot{S} = -SA - A^T S + SBS - C \tag{31}$$

$$\dot{R} = -(A^T - SB)R \tag{32}$$

$$\dot{Q} = R^T B R \tag{33}$$

and the boundary conditions

$$S(t_f) = \left[\phi_{\boldsymbol{xx}} + \left(\boldsymbol{\nu}^T \psi_{\boldsymbol{x}} \right)_{\boldsymbol{x}} \right]_{t=t_f} \tag{34}$$

$$R(t_f) = \left[\psi_{\boldsymbol{x}}^T \right]_{t=t_f} \tag{35}$$

$$Q(t_f) = 0 \tag{36}$$

Through algebraic manipulations, Eqs. (29) and (30) can be combined and substituted back into Eq. (23) to yield an expression of $\delta \boldsymbol{u}(t)$ in the form of a feedback law using the offset from the optimal trajectory $\delta \boldsymbol{x}$ and the desired terminal condition offset $\delta\psi$ as inputs:

$$\delta \boldsymbol{u}(t) = -H_{uu}^{-1}\left\{\left[H_{ux} + f_u^T(S - RQ^{-1}R^T)\right]\delta \boldsymbol{x}(t) + f_{\boldsymbol{u}}^T RQ^{-1}\delta\psi\right\} \tag{37}$$

Thus, once $S(t)$, $R(t)$, and $Q(t)$ are solved for the complete trajectory, Eq. (37) becomes a feedback control that leads to the reference terminal conditions or any small offset from these conditions (if desired) while minimizing the cost function J.

III. Application to Formation Flight

The next step is to apply this theory to the formation-flying control problem. Let $\boldsymbol{e} = [a/R_e \;\; e \;\; i \;\; \Omega \;\; \omega \;\; \nu]^T$ be the state vector, where a/R_e is the orbit semimajor axis normalized by Earth equatorial radius, e is the orbit eccentricity, i is the orbit inclination, Ω is the right ascension of the ascending node, ω is the argument of perigee, and ν is the true anomaly. The system dynamics f are derived from the Gauss variational equations:

$$f = \begin{bmatrix} \frac{2a^2}{R_e h}\left(e\sin(\nu)u_r + \frac{p}{r}u_t\right) \\ \frac{1}{h}\{p\sin(\nu)u_r + [(p+r)\cos(\nu) + re]u_t\} \\ \frac{r\cos(\theta)}{h}u_h \\ \frac{r\sin(\theta)}{h\sin(i)}u_h \\ \frac{1}{he}(-p\cos(\nu)u_r + (p+r)\sin(\nu)u_t) - \frac{r\sin(\theta)\cos(i)}{h\sin(i)}u_h \\ \frac{h}{r^2} + \frac{1}{he}[p\cos(\nu)u_r - (p+r)\sin(\nu)u_t] \end{bmatrix} \tag{38}$$

where h is the orbit angular momentum, p is the semilatus rectum, r is the spacecraft distance from the Earth center, θ is the argument of latitude, and $\boldsymbol{u} = [u_r \;\; u_t \;\; u_h]^T$ is the control vector, with its elements being the control accelerations in the radial, transverse, and normal directions, respectively. The previous equation contains singularities for circular or equatorial orbits. Hence, as formulated here, the controller is only applicable to inclined elliptical orbits. To be applicable to circular, near-circular, or equatorial orbits, the system would have to be recast in terms of nonsingular elements. Several publications already cover the problem of optimal control for circular orbits [3,9].

The cost function is designed to minimize both the quadratic control effort $\boldsymbol{u}^T\boldsymbol{u}$ and the quadratic relative orbit element error $(\Delta \boldsymbol{e})^T\Delta \boldsymbol{e}$. Therefore,

$$L = \tfrac{1}{2}\boldsymbol{u}^T(\mathrm{diag}[\,\rho_r \quad \rho_t \quad \rho_h\,])\boldsymbol{u} = \tfrac{1}{2}\boldsymbol{u}^T\rho\boldsymbol{u} \tag{39}$$

$$\begin{aligned}\phi(t_f) &= \tfrac{1}{2}\boldsymbol{\Delta e}^T(\mathrm{diag}[\,K_a \quad K_e \quad K_i \quad K_\Omega \quad K_\omega \quad K_\nu\,])\boldsymbol{\Delta e} \\ &= \tfrac{1}{2}\boldsymbol{\Delta e}^T K\boldsymbol{\Delta e}\end{aligned} \tag{40}$$

where ρ and K are weighting matrices.

It has been decided to implement a cost to a final state error: that is, with $\phi \neq 0$ in Eq. (1) rather than imposing terminal conditions [i.e., $\psi(t_f) = 0$]. This is to provide more freedom to the controller in the minimization of the cost. Indeed, the controller will thus be able to sacrifice the accuracy of the formation to minimize the propellant consumption, but always based on the relative values of K and ρ. An infinite value of K is theoretically identical to imposing a desired final state vector.

The only remaining missing information to synthesize the controller is the time evolution of the reference states and the Lagrange multipliers for the optimal (or nominal) trajectory. The problem is largely simplified if one assumes that the trajectory of the leader (the reference trajectory) is uncontrolled and follows its natural motion. This does not mean that the elements of the formation have to remain uncontrolled, but rather that all of the elements of the formation evolve around an uncontrolled reference orbit, which could be either another spacecraft or a virtual point in space. This is a desirable scenario to maximize the lifetime of a formation-flying mission, because all spacecraft evolve close to a trajectory that does not require any control effort to maintain.

The required accuracy of the uncontrolled reference trajectory's orbit prediction method varies with the planned duration of the maneuver. For small-duration maneuvers (1–2 orbits), unperturbed Keplerian dynamics are sufficiently accurate, because this trajectory is only used to compute the controller gains. However, over a longer time frame, the reference trajectory itself could be substantially in error with respect to the true uncontrolled motion if the model is not accurate enough. This would cause the controller gains to no longer be synchronized with the current orbital dynamics. For longer maneuvers, orbit propagation methods that take into account the J_2 zonal harmonic or other relevant perturbations should be considered. For the sake of simplicity, only an unperturbed model of motion is used here for the computation of the controller gain S.

If the reference trajectory is uncontrolled, the dynamics of the states are decoupled from the Lagrange multipliers dynamics. Indeed, for an uncontrolled reference trajectory, $L_{\boldsymbol{u}} = \rho\boldsymbol{u} = 0$, and so enforcing Eq. (11) yields

$$\boldsymbol{\lambda}(t) = 0 \tag{41}$$

which means that the Hamiltonian of the system is only a function of $\boldsymbol{u}$. Consequently, all of the derivatives of H with respect to $\boldsymbol{x}$ are 0,

$$H_{\boldsymbol{ux}} = 0 \tag{42}$$

$$H_{\boldsymbol{xu}} = 0 \tag{43}$$

$$H_{\boldsymbol{xx}} = 0 \tag{44}$$

and its second-order derivative is constant:

$$H_{\boldsymbol{uu}} = \rho \tag{45}$$

Also, because $\psi(t_f) = 0$ and $\delta\psi = 0$,

$$R(t) = 0 \tag{46}$$

$$Q(t) = 0 \tag{47}$$

which leaves us with only S as an unknown in Eq. (37). When substituting these new results, Eq. (37) is reduced to its simplified form:

$$\delta \boldsymbol{u}(t) = -H_{\boldsymbol{uu}}^{-1} f_{\boldsymbol{u}}^T S(t)\delta \boldsymbol{x}(t) \tag{48}$$

From the dynamics of the system of Eq. (38), $f_{\boldsymbol{u}}$ is

$$f_{\boldsymbol{u}} = \begin{bmatrix} \frac{2a^2 e\sin\nu}{hR_e} & \frac{2a^2 p}{hrR_e} & 0 \\ \frac{p\sin\nu}{h} & \frac{(p+r)\cos\nu + re}{h} & 0 \\ 0 & 0 & \frac{r\cos\theta}{h} \\ 0 & 0 & \frac{r\sin\theta}{h\sin i} \\ -\frac{p\cos\nu}{he} & \frac{(p+r)\sin\nu}{he} & -\frac{r\sin\theta\cos i}{h\sin i} \\ \frac{\eta(p\cos\nu - 2re)}{he} & -\frac{\eta(p+r)\sin\nu}{he} & 0 \end{bmatrix} \tag{49}$$

Moreover, because the reference trajectory is uncontrolled ($\boldsymbol{u} = 0$), $f_{\boldsymbol{x}}$ takes the simple form:

$$f_x = -\frac{n(1+e\cos\nu)}{\eta^3}\begin{bmatrix} 0 & 0 & 0 & 0 & 0 & 0 \\ 0 & 0 & 0 & 0 & 0 & 0 \\ 0 & 0 & 0 & 0 & 0 & 0 \\ 0 & 0 & 0 & 0 & 0 & 0 \\ 0 & 0 & 0 & 0 & 0 & 0 \\ \frac{-3R_e(1+e\cos\nu)}{2a} & e^2\cos\nu + 3e + 2\cos\nu & 0 & 0 & 0 & 2e\sin\nu \end{bmatrix} \tag{50}$$

With all these simplifications, Eq. (31) becomes

$$\dot{S} = -Sf_x - f_x^T S + \left(Sf_u\right)H_{uu}^{-1}\left(f_u^T S\right) \tag{51}$$

with the final conditions

$$S(t_f) = K \tag{52}$$

From the form of Eqs. (51) and (52), S is obviously a 6×6 symmetric matrix if K is symmetric (which is the case in the current application). This means that Eq. (51) is a system of 21 coupled differential equations, for which it seems unlikely to get an analytical solution. However, Eq. (51) can be integrated numerically backward from t_f to t_0, and the time evolution of $S(t)$ can be stored onboard because $S(t)$ only depends on the initial (or the final) location of the reference trajectory and the duration of the maneuver.

Once $S(t)$ is solved, Eq. (37) becomes a feedback law that can be applied on all of the elements of the formation. Because the reference is uncontrolled, the command increment $\delta\boldsymbol{u}(t)$ becomes the command $\boldsymbol{u}(t)$ to apply to each element of the formation:

$$\boldsymbol{u}(t) = -\rho^{-1} f_u^T S(t)\Delta\boldsymbol{e}(t) \tag{53}$$

where the orbit element error $\Delta\boldsymbol{e}(t)$ is the difference between the current relative orbit element vector $\delta\boldsymbol{e}(t)$ and the desired relative orbit elements $\delta\boldsymbol{e}_d(t)$. This control law minimizes both the fuel consumption and the final orbit element error $\Delta\boldsymbol{e}$ through the minimization of the cost function J. Thus, the selection of the values of K and ρ is a way of performing the tradeoff between formation accuracy and propellant consumption.

Finally, the stability conditions of this controller are discussed. Because of the semi-analytic nature of the controller, it is difficult to demonstrate the stability of the controller under any conditions. However, it is possible to assess under which conditions the stability of the control law can be verified. This can be done by looking at the conditions under which a Lyapunov function for the error dynamics exists. As stated by the Lyapunov stability theory for non-autonomous systems, a sufficient condition for the controlled system to be uniformly globally asymptotically stable is the existence of a decrescent and radially unbounded Lyapunov function for the system [12]. Let V be a Lyapunov function for the error dynamics [1]:

$$V(\Delta\boldsymbol{e}, t) = \tfrac{1}{2}(\alpha_1 + \alpha_2 e^{-\lambda t})\Delta\boldsymbol{e}^T\Delta\boldsymbol{e} \tag{54}$$

where α_1, α_2, and λ are positive scalars. The proposed function is positive-definite because there exists a time-invariant positive-definite function $V_0(\Delta\boldsymbol{e})$ such that

$$V(\Delta\boldsymbol{e}, t) \geq \frac{\alpha_1}{2}\Delta\boldsymbol{e}^T\Delta\boldsymbol{e} = V_0(\Delta\boldsymbol{e}) \tag{55}$$

Moreover, the function $V(\Delta\boldsymbol{e}, t)$ is decrescent because there exists a time-invariant positive-definite function V_1 such that

$$V(\Delta\boldsymbol{e}, t) \leq \frac{\alpha_1 + \alpha_2}{2}\Delta\boldsymbol{e}^T\Delta\boldsymbol{e} = V_1(\Delta\boldsymbol{e}) \tag{56}$$

Finally, $V(\Delta\boldsymbol{e}, t)$ is radially unbounded because $V(\Delta\boldsymbol{e}, t) \to \infty$ as $\Delta\boldsymbol{e} \to \infty$.

Assuming that the system is unperturbed, the error dynamics are

$$\Delta\dot{\boldsymbol{e}} = f_x\Delta\boldsymbol{e} + f_u\boldsymbol{u} \tag{57}$$

From Eqs. (53) and (57), the Lyapunov function rate becomes

$$\dot{V}(\Delta\boldsymbol{e}, t) = -\frac{\alpha_2\lambda}{2}\Delta\boldsymbol{e}^T\Delta\boldsymbol{e} + (\alpha_1 + \alpha_2 e^{-\lambda t})\Delta\boldsymbol{e}^T\Delta\dot{\boldsymbol{e}} \tag{58}$$

$$\dot{V}(\Delta\boldsymbol{e}, t) = -\frac{\alpha_2\lambda}{2}\Delta\boldsymbol{e}^T\Delta\boldsymbol{e} - (\alpha_1 + \alpha_2 e^{-\lambda t})\Delta\boldsymbol{e}^T \times \left(\rho^{-1} f_u f_u^T S - f_x\right)\Delta\boldsymbol{e} \tag{59}$$

To conclude on the stability of the system, the function $\dot{V}(\Delta\boldsymbol{e}, t)$ needs to be negative-definite. Thus, the controlled system is globally asymptotically stable if the matrix $(\rho^{-1} f_u f_u^T S - f_x)$ is positive-definite. The stability of the controller can therefore be assessed before the maneuver, because the values of ρ, S, f_u, and f_x are known beforehand. Note that this is a sufficient condition for stability, not a necessary condition. If the product $(\rho^{-1} f_u f_u^T S - f_x)$ is not positive-definite for the complete trajectory, further investigation is required to assess the stability of the controller.

However, more simple stability conditions can be derived assuming that the controller gains S and ρ^{-1} are sufficiently large. If this is the case, $\rho^{-1} f_u f_u^T S \gg f_x$ and f_x can be dropped with respect to $\rho^{-1} f_u f_u^T S$. Hence, the stability condition is limited to $\rho^{-1} f_u f_u^T S$ being positive-definite. The matrix ρ^{-1} is assumed to be the identity matrix or the identity matrix multiplied by a positive gain. Under this circumstance, the condition for stability can be redefined as $(f_u f_u^T)S$ being positive-definite. Because both $f_u f_u^T$ and S are symmetric, $(f_u f_u^T)S = S(f_u f_u^T)$, which means that the product is positive-definite if and only if both $f_u f_u^T$ and S are positive-definite. This leaves us with the conclusion that the controller is globally stable if the gain matrix $S(t)$ is positive-definite for $t_0 \leq t \leq t_f$. Once again, this is a sufficient condition for stability, not a necessary condition. For low-Earth-orbit formations, the order of magnitude of the terms of f_x and f_u is 10^{-2} or smaller. This means that the order of magnitude of the product $f_u f_u^T$ is 10^{-4}. Hence, the norm of the product $\rho^{-1} S$ should be of at least 10^4 throughout the maneuver for this simplifying assumption to hold.

This algorithm is well suited for reconfiguration maneuvers, as it will only associate an importance to the final relative orbit elements error. It can locally sacrifice formation accuracy to save propellant for moments of the maneuver in which propellant will be efficient, as it is aware of the dynamics of the system through f_u and S. Other types of controllers such as the LQR or the mean orbit element controller only have a limited knowledge of the dynamics of the system and have no notion of the duration of the maneuver. They therefore cannot guarantee optimality (or suboptimality) of the reconfiguration. However, the neighboring optimum feedback law developed here is not fully analytical. An analytical version of this feedback controller would require an analytical solution to $S(t)$, which seems very difficult to obtain, if at all possible. Because its computation assumes unperturbed motion of the reference trajectory, it is only a function of the controller weights K and ρ, the initial position of the reference at the beginning of the trajectory, and the duration of the maneuver. Therefore, whatever the number of spacecraft in the formation, $S(t)$ only needs to be solved once and the

controller guarantees a near-optimal result for all of the members of the formation, as long as they remain sufficiently close to the uncontrolled reference trajectory.

IV. Simulation Results

In this section, we shall compare the neighboring optimal feedback law with other common formation-flying control algorithms: namely, a traditional LQR and the mean orbit elements controller. Results shall be compared for a typical formation-flying problem: the reconfiguration from an arbitrary location into a projected-circular formation (PCF) performed over a duration of one orbit. Two simulation scenarios are considered: a small eccentricity orbit and a highly elliptical orbit.

The reference, or chief, initial orbit elements $\boldsymbol{e}_0$ for the first simulation scenario are given in Table 1. This reference orbit starts from the initial states of Table 1 and follows a natural uncontrolled motion until the end of the maneuver one orbit later. The deputy spacecraft that performs the maneuver starts with the relative state vector $\delta\boldsymbol{e}_0$, as described in Table 2. The relative orbit elements of the deputy $\delta\boldsymbol{e}$ is the difference between the orbit elements of the deputy $\boldsymbol{e}_d$ and the orbit elements of the chief $\boldsymbol{e}_c$. It shall be noted that in this section, relative motion is described in terms of relative mean anomaly δM, instead of relative true anomaly $\delta\nu$. This is common in the formation-flying literature because relative mean anomaly remains naturally constant for unperturbed and uncontrolled orbits with the same orbital energy. However, the neighboring optimum feedback controller applied later in this section still expects a true anomaly error as input, as the dynamic model used in the computation of the controller gains uses ν as the sixth state variable.

The final reference orbit elements after one orbit are given in Table 3. These elements are the result of a one-orbit propagation considering the effect of J_2 perturbations. The final desired relative orbit elements of the deputy are given in Table 4. These relative states would locally place the deputy on a 1 km PCF around the reference trajectory. The control problem therefore consists of maneuvering the deputy from $\delta\boldsymbol{e}_0$ to $\delta\boldsymbol{e}_f$ at $t_f = 5840$ s (i.e., one orbit later).

Table 1 Chief initial orbit elements $\boldsymbol{e}_0$ for simulation scenario 1

a_0	$1.1R_e$
e_0	0.05
i_0	$\pi/4$ rad
Ω_0	0
ω_0	0
M_0	0

Table 2 Deputy initial orbit elements $\delta\boldsymbol{e}_0$ offset for simulation scenario 1

δa_0	0
δe_0	+0.0001
δi_0	+0.0001 rad
$\delta\Omega_0$	−0.0001 rad
$\delta\omega_0$	−0.0001 rad
δM_0	+0.0001 rad

Table 3 Chief final orbit elements $\boldsymbol{e}_f$ for simulation scenario 1

a_f	$1.1R_e$
e_f	0.05
i_f	$\pi/4$ rad
Ω_f	−0.0060 rad
ω_f	0.0065 rad
M_f	0 rad

Table 4 Deputy desired orbit elements $\delta\boldsymbol{e}_f$ offset after 1 orbit for simulation scenario 1

δa_f	−87.98 m
δe_f	2.57×10^{-5}
δi_f	1.1564×10^{-4} rad
$\delta\Omega_f$	-1.0819×10^{-4} rad
$\delta\omega_f$	−0.0010 rad
δM_f	0.0011 rad

The first controller with which the neighboring optimum feedback law is compared is the conventional LQR controller. This controller is designed to use the Hill coordinates (relative position and velocity in the orbital frame) as inputs and then to output a control acceleration in the orbital frame. It is synthesized using the linearized CWH model of relative motion, which can be written as

$$\begin{bmatrix} \dot{\boldsymbol{x}} \\ \dot{\boldsymbol{V}} \end{bmatrix} = \begin{bmatrix} 0 & 0 & 0 & 1 & 0 & 0 \\ 0 & 0 & 0 & 0 & 1 & 0 \\ 0 & 0 & 0 & 0 & 0 & 1 \\ 3n^2 & 0 & 0 & 0 & 2n & 0 \\ 0 & 0 & 0 & -2n & 0 & 0 \\ 0 & 0 & -n^2 & 0 & 0 & 0 \end{bmatrix} \begin{bmatrix} \boldsymbol{x} \\ \boldsymbol{V} \end{bmatrix} \tag{60}$$

where n is the orbital mean motion of the chief and $\boldsymbol{x}$ and $\boldsymbol{V}$ are, respectively, the relative position and velocity in the radial, transverse, and normal directions. Obviously, the CWH model assumes a circular reference orbit, which will inevitably affect the performance of the controller in this nonzero eccentricity simulation scenario. Nevertheless, the LQR represents one of the simplest controllers that can be implemented in this context and can be used as a reference. This infinite-horizon type of controller seeks to minimize the cost function:

$$J = \int_0^\infty [(\Delta\boldsymbol{x})^T Q(\Delta\boldsymbol{x}) + \boldsymbol{u}^T R\boldsymbol{u}]\mathrm{d}t \tag{61}$$

where $\Delta\boldsymbol{x}$ is the position and velocity error vector and Q and R are weighting matrices. In this particular scenario, Q was set as the identity matrix and R is a diagonal matrix with 10^9 as nonzero elements. The result is a static gain matrix K that computes the control commands from the Hill coordinates errors:

$$\boldsymbol{u} = -K\Delta\boldsymbol{x} \tag{62}$$

The second benchmark controller is the mean orbit elements controller [1,5]. As opposed to the LQR, the mean orbit elements controller uses orbit element errors as input. The control of orbit elements instead of Hill coordinates provides the main advantage of having a controller that more wisely uses the laws of orbital dynamics. By having some gains high or low at certain points of the orbit, it is possible to correct some orbit element errors at a location at which the control command is efficient. In one of its simplest forms, the mean orbit elements controller can be expressed as

$$\boldsymbol{u} = -P\left(f_{\boldsymbol{u}}^T f_{\boldsymbol{u}}\right)^{-1} f_{\boldsymbol{u}}\Delta\boldsymbol{e} \tag{63}$$

The matrix P is a time-varying gain matrix. The only constraint in the demonstration of the stability of this controller is for P to be positive-definite and sufficiently large [1]. We choose here to define P as

$$P = I\begin{bmatrix} P_{a_0} + P_{a_1}\cos^N\frac{\nu}{2} \\ P_{e_0} + P_{e_1}\cos^N\nu \\ P_{i_0} + P_{i_1}\cos^N\theta \\ P_{\Omega_0} + P_{\Omega_1}\sin^N\theta \\ P_{\omega_0} + P_{\omega_1}\sin^N\nu \\ P_{M_0} + P_{M_1}\sin^N\nu \end{bmatrix} \tag{64}$$

Two heuristics were tried to optimize the controller gains. The first one consisted of systematically and independently increasing each of

the 12 gains (all of the others were set to 0) up to the point at which an increase in velocity impulse did not provide any significant reduction of the final error. The second method consisted of imposing a single value for the P_0 vector and another value to the P_1 vector terms. In this case, the P_0 and the P_1 gains were independently increased (forcing the other vector to 0) until an increase in velocity impulse did not cause any significant decrease of the final error. The latter case provided the best results in this particular simulation scenario. The values of the coefficients of the P matrix were set to

$$P_{a_0} = P_{e_0} = P_{i_0} = P_{\Omega_0} = P_{\omega_0} = P_{M_0} = 0.001$$

$$P_{a_1} = P_{e_1} = P_{i_1} = P_{\Omega_1} = P_{\omega_1} = P_{M_1} = 0.001$$

and $N = 6$. The value for N was optimized based on these values of P_0 and P_1. This set of gains provided the best performance that could be achieved by the authors with this controller for the desired maneuver over a one-orbit period. The set of gains proposed in the original mean orbit element controller work [5], tuned for a slightly larger orbit ($a = 7555$ km, $e = 0.05$, $i = 48$ deg, $\Omega = 0$, $\omega = 10$ deg, and $M = 120$ deg), led to a tenfold increase of the final quadratic error for 4 times the fuel cost when compared with the gain set proposed here. Hence, the selection of the optimal values of these 13 variables is within itself a very challenging task [5]. As of now, there is no systematic way of identifying the optimal gain values for the mean orbit elements controller other than independently tuning each of the 13 parameters. Moreover, as it has been noted in this particular scenario, the optimal values for the gains largely depend on the orbital parameters and the targeted duration for the maneuver.

Finally, for the neighboring optimum feedback law, $S(t)$ was computed offline and then stored. Once the trajectory of the reference is predicted, Eq. (51) is solved using Eq. (52) as boundary conditions. The values of the weighting matrices, which are the only values to tune in the controller, were set to

$$K = 10^6 \cdot I \tag{65}$$

$$\rho = I \tag{66}$$

In simulation, the value for S at each time step is interpolated from a lookup table. A block-scheme representation of the implementation of the controller is given in Fig. 1. As shown in this figure, the only inputs required are the current orbit element vector of the deputy $\boldsymbol{e}_d$, the desired set of elements $\boldsymbol{e}_{\text{des}}$, and the current maneuver time t required to interpolate the value of $S(t)$. Formally speaking, the chief orbit elements $\boldsymbol{e}_c$ should be used to compute $f_{\boldsymbol{u}}^T$ instead of the deputy state vector in Eq. (53). However, because the absolute orbit elements of the chief and the deputy are so close, there is no numerically significant difference between $f_{\boldsymbol{u}}(\boldsymbol{e}_c)$ and $f_{\boldsymbol{u}}(\boldsymbol{e}_d)$. The use of one or the other in the computation of $f_{\boldsymbol{u}}^T$ has virtually no impact on the performance of the controller. To use $\boldsymbol{e}_d$ instead reduces the number of inputs of the controller.

For all three control algorithms, the desired trajectory $\delta\boldsymbol{e}_{\text{des}}(t)$, from which the error is computed, is the trajectory that would naturally (i.e., without any control effort) lead to the desired position at time t_f. This trajectory can be computed with any state-transition matrix that predicts relative motion in the form

$$\delta\boldsymbol{e}_{\text{des}}(t) = \Phi^{-1}(t)\delta\boldsymbol{e}_f \tag{67}$$

where $\Phi(t)$ is a matrix that maps the current relative orbit elements to the set of relative orbit elements at time t_f. In simulation, a model for J_2-perturbed elliptical orbits linearized about the reference trajectory was used [13,14]. Therefore, once the error between $\delta\boldsymbol{e}$ and $\delta\boldsymbol{e}_{\text{des}}$ is reduced to zero, no further control effort is required to bring the spacecraft to its desired location at $t = t_f$.

The resulting control command history for each of the controllers is given in Figs. 2–4 (each figure uses a different scale to highlight the command history profile). The time history of the magnitude of the command signal history for all control (CTL) laws is shown in Fig. 5.

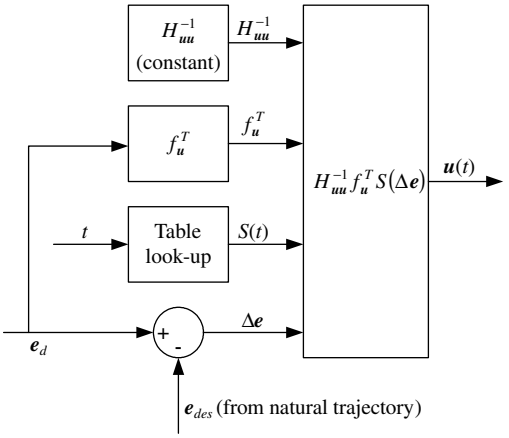

Fig. 1 Block scheme of the neighboring optimum feedback law implementation.

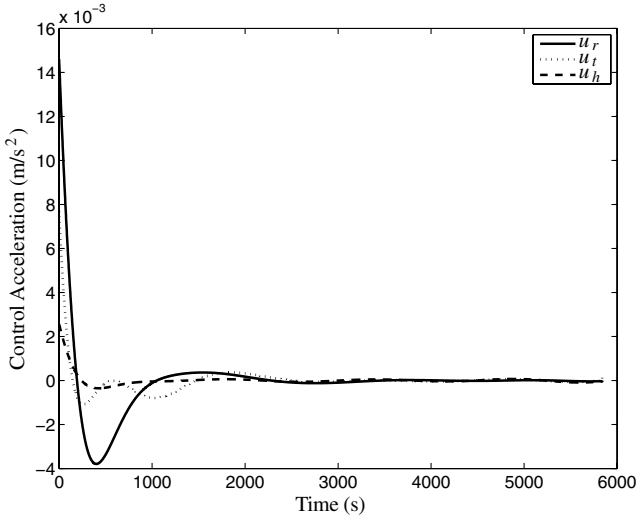

Fig. 2 LQR command signal history for simulation scenario 1.

The time history of the quadratic error $\Delta\boldsymbol{e}^T\Delta\boldsymbol{e}$ between the desired natural trajectory and the actual trajectory for each controller is shown in Fig. 6. A comparison of the fuel cost (total required velocity impulse), the quadratic effort U,

$$U = \int_{t_0}^{t_f} (\boldsymbol{u}^T\boldsymbol{u})\mathrm{d}t \tag{68}$$

and the final error for each of the algorithms is presented in Table 5.[‡] The algorithms are also compared with the optimal control theory open-loop solution [11] when imposing the final desired orbit elements as constraints to the problem and minimizing the quadratic control effort U. This type of controller is not a feedback controller. However, it is used here as a baseline because it provides the optimal solution, assuming that both modeled dynamics and true dynamics are similar.

As can be seen in Table 5, the neighboring optimum feedback law provides better accuracy (in terms of final quadratic error) than the two other controllers with a smaller fuel cost (both in terms of total absolute velocity impulse and total quadratic effort). The reader should note, however, that this is not a control algorithm comparison campaign. It could be possible to obtain slightly better performance with the other two algorithms with more finely tuned gains. However, it is the authors' opinion that the simulation results

[‡]Simulations were performed assuming J_2-perturbed dynamics with a 1/200 orbital period fundamental step size, fixed-step ode4 Simulink version 6.4 solver, and 10^{-6} absolute error tolerance.

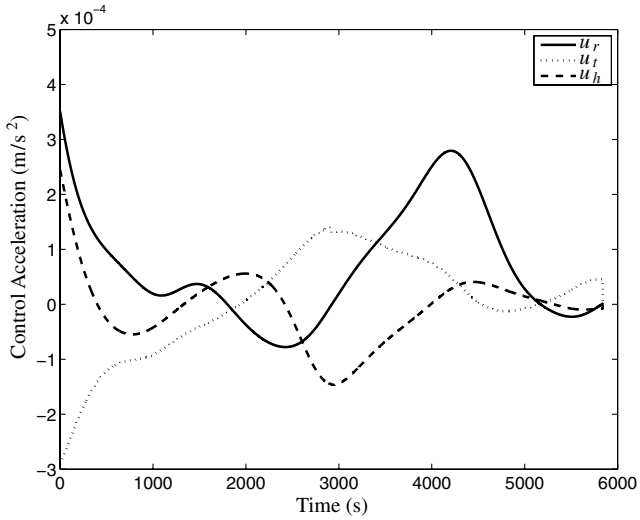

Fig. 3 Mean orbit elements controller command signal history for simulation scenario 1.

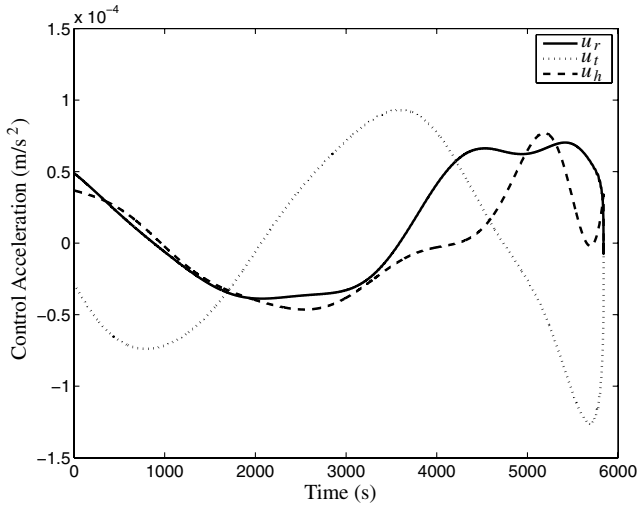

Fig. 4 Neighboring optimum feedback controller command history for simulation scenario 1.

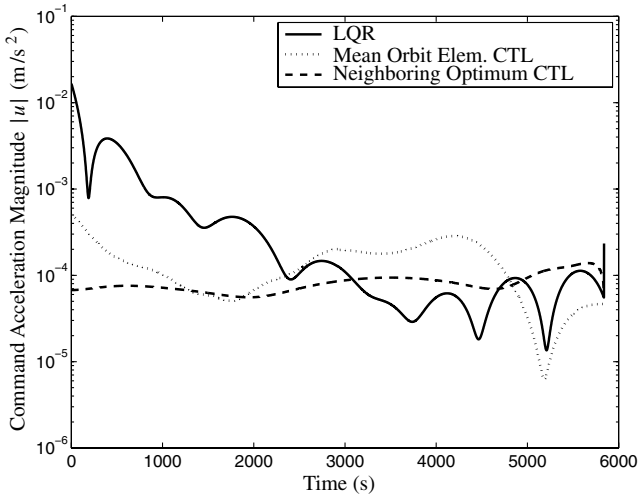

Fig. 5 Feedback controller command signal magnitude history for simulation scenario 1.

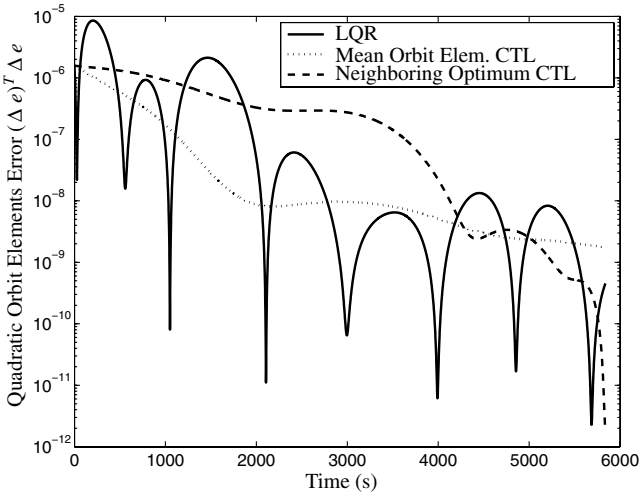

Fig. 6 Orbit element quadratic error time history for simulation scenario 1.

presented here are typical of what can be expected from the controllers. Therefore, these results are used as an indicator of relative performance.

By looking at Figs. 2–5, the reader shall note that the neighboring optimum feedback law has a relatively constant but small command magnitude, whereas the two other feedback controllers have higher command acceleration magnitudes. This is especially true for the LQR that tries to correct the error right from the start and maintains a large steady-state error (approximately 10^{-8}) for the remaining minutes of the maneuver. This steady-state error is inevitable because of the elliptical nature of the reference orbit (the LQR design assumed a circular reference orbit) and the presence of perturbations caused by J_2 harmonics. The neighboring optimum feedback law is the only controller out of the three that is able to sacrifice formation accuracy at the beginning of the trajectory to get payoffs in terms of propellant and accuracy at the moment at which the formation is needed.

As the simulations show, the neighboring optimum controller is not suited for the case in which the tracking error is to remain small throughout the maneuver. The proposed neighboring optimum controller only reduces the tracking error at the final time, disregarding the tracking error before the targeted point. In turn, both the LQR and the mean orbit elements controller aim at reducing the error throughout the maneuver (not only at final time), which can partly justify their increased fuel cost. However, the reference trajectory is such that if the tracking error were to be perfectly corrected at a given instant, no further control effort would be required. Therefore, maintaining a small tracking error should not be expensive in terms of fuel cost in that particular scenario. It should also be noted that the mean orbit element controller, as the name says, tracks mean orbit element errors. The controller disregards short-period oscillations of the osculating elements, which could explain the residual orbit element errors computed in terms of relative osculating orbit elements.

It is also interesting to observe that the neighboring optimal feedback law basically recreates the optimal open-loop command, which once again demonstrates the near-optimality of the neighboring optimum feedback law. As can be seen in Fig. 7, the time history of the optimal open-loop command is similar to the output computed by the feedback law, especially during the first part of the trajectory. This explains why the performance in terms of fuel consumption of the neighboring optimum feedback law is so close to the performance of the open-loop optimal command computed offline. The slight difference that remains between the neighboring optimal control law and the open-loop control signal has essentially two sources. First, the neighboring optimum controller solution is a linearization of the optimal solution. There is inevitably a linearization error. Second, the feedback controller is not aware of the presence of the J_2 harmonic, whereas the optimal control signal is

Table 5 Comparison of the algorithm simulation results for simulation scenario 1

	LQR	Mean orbit elements controller	Neighboring optimum feedback controller	Open-loop optimal command
Fuel cost, m/s	3.9324	0.8181	0.4770	0.4721
Quadratic control effort, m^2/s^3	0.0186	1.6363×10^{-4}	4.1250×10^{-5}	4.0851×10^{-5}
Quadratic final error	4.5376×10^{-10}	1.7918×10^{-9}	2.0837×10^{-12}	0

Table 6 Chief initial orbit elements e_0 for simulation scenario 2

a_0	27,512 km
e_0	0.75
i_0	$\pi/4$ rad
Ω_0	0
ω_0	0
M_0	π

Table 7 Chief final orbit elements e_f for simulation scenario 2

a_f	27,501 km
e_f	0.7499
i_f	0.7854 rad
Ω_f	−0.0020 rad
ω_f	0.0024 rad
M_f	π rad

computed with J_2-perturbed dynamics. This demonstrates that the controller can provide near-optimal results even in the presence of perturbations of the importance of the J_2 harmonic.

The second simulation scenario is a 500-km-alt perigee highly elliptical orbit, as described in Table 6. In this test case, the formation starts from apogee and is to achieve a PCF formation exactly one orbit later (i.e., at the next apogee). Such a maneuver is typical of some sun observation missions, such as the ESA PROBA-3 mission. The initial location of the deputy is similar to the first test scenario (Table 2). The final location of the chief, 1 orbit (45,416 s) later is given in Table 7. The targeted deputy final orbital element offset is given in Table 8.

Figures 8 and 9 present the command signal history and the quadratic error time history for both the mean orbit element controller and the neighboring optimum controller. The mean orbit element controller gains were tuned for this particular scenario with the method described earlier. The optimal values of the P matrix were found to be

Table 8 Deputy desired orbit elements δe_f offset after 1 orbit for scenario 2

δa_f	−309.0 m
δe_f	3.582×10^{-5}
δi_f	3.503×10^{-4} rad
$\delta\Omega_f$	-2.593×10^{-5} rad
$\delta\omega_f$	1.401×10^{-6} rad
δM_f	3.434×10^{-5} rad

$$P_{a_0} = P_{e_0} = P_{i_0} = P_{\Omega_0} = P_{\omega_0} = P_{M_0} = 1 \times 10^{-4}$$

and

$$P_{a_1} = P_{e_1} = P_{i_1} = P_{\Omega_1} = P_{\omega_1} = P_{M_1} = 0$$

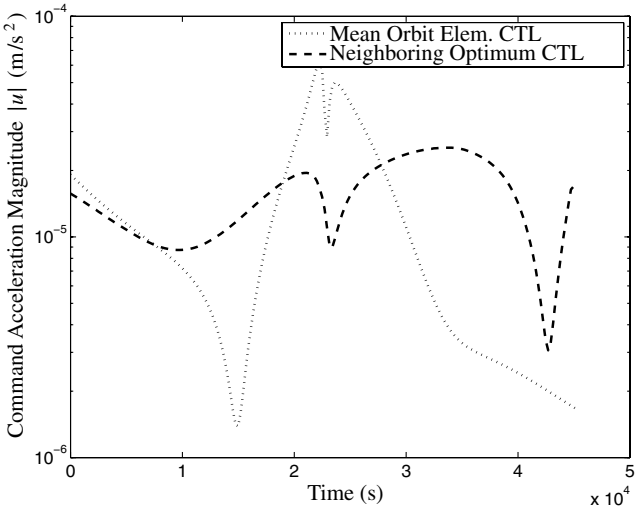

Fig. 8 Feedback controllers command signal magnitude history for simulation scenario 2.

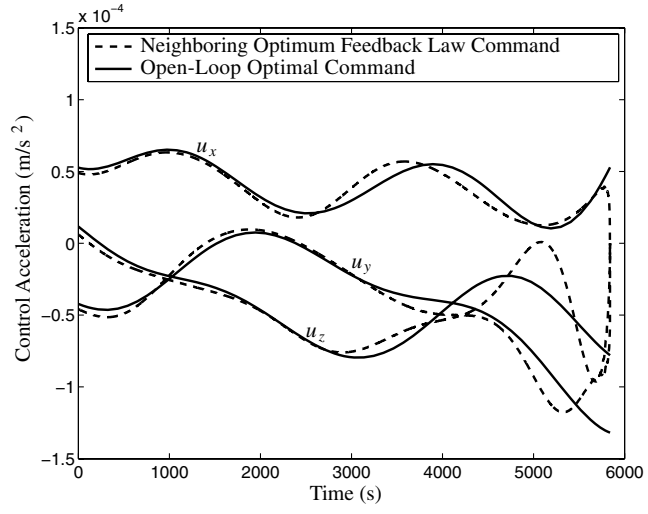

Fig. 7 Components of the command acceleration in the inertial frame for simulation scenario 1.

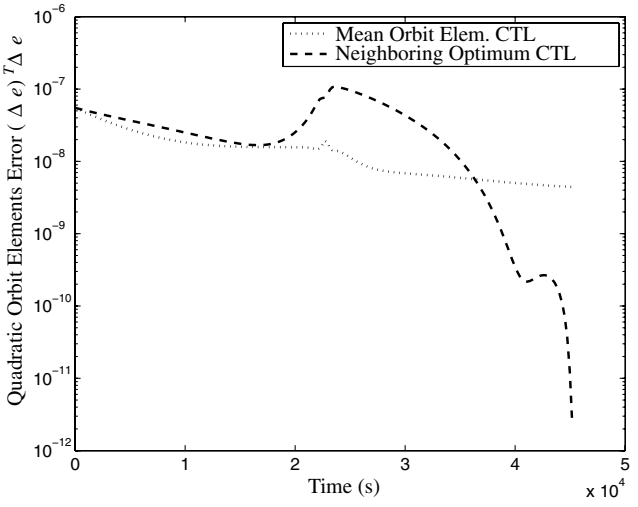

Fig. 9 Orbit element quadratic error time history for simulation scenario 2.

Table 9 Comparison of the algorithm simulation results for simulation scenario 2

	Mean orbit elements controller	Neighboring optimum feedback controller
Fuel cost, m/s	0.5268	0.5835
Quadratic control effort, m^2/s^3	1.329×10^{-5}	8.678×10^{-6}
Quadratic final error	4.425×10^{-9}	2.326×10^{-12}

The LQR was not used as a basis of comparison for this simulation scenario because of its poor control performance for time-varying relative motion dynamics such as highly elliptical orbits. The gains for the neighboring optimum controller synthesis are similar to those of simulation scenario 1.

As Fig. 8 shows, the mean orbit element controller waits for the perigee to perform the relative semimajor-axis error correction, which explains the large peak in command acceleration magnitude in the middle of the maneuver and the corresponding decrease in orbital element error past the perigee. The neighboring optimum controller, however, spreads this correction over a longer duration to avoid command peaks and minimize the quadratic control effort. Both mean orbit elements controller and neighboring optimum controller show quite similar fuel consumption to perform the maneuver (lower mean orbit elements controller ΔV cost but larger quadratic control effort) whereas the final neighboring optimum controller error is 3 orders of magnitude smaller (Table 9). Once again, as Fig. 9 shows, this increased performance is at the expense of an error that remains large until the last moments of the maneuver.

As can be noted in Figs. 6 and 9, the error dynamics of the neighboring optimum controller are similar in both scenarios. In both cases, the error stagnates (or even increases) during the first moments of the maneuver but drops close to the end of the maneuver. These simulations thus show that the neighboring optimum controller yields good performance for highly elliptical orbits as well.

V. Conclusions

This paper shows how results of the optimal control theory can be applied to formation flight to get a neighboring optimum feedback law. The controller is of the semi-analytical form, as only one time-varying gain matrix needs to be numerically computed. However, once this matrix is known, the controller provides essentially optimal results for all of the elements of the formation, assuming that they orbit sufficiently close to the uncontrolled reference trajectory. The controller shows good performance with small and large eccentricity orbits. This type of controller is suited for onboard implementation in which snapshot types of formation are needed (i.e., when a specific formation is needed at a specific point of the orbit), disregarding the formation accuracy during the maneuver.

The performance of this controller has been compared with two other common formation-flying controllers: namely, the LQR and the mean orbit elements controller in a typical PCF reconfiguration problem. The proposed neighboring optimum feedback law yielded a better accuracy while maintaining a similar or smaller fuel consumption, both in terms of absolute velocity impulse and quadratic control effort.

Future work on the controller would be to identify solution paths to obtain an analytical solution to the S matrix or under which assumptions such a solution can be obtained. This would lead to a fully analytical feedback control law that guarantees near-optimality for all of the members of the formation. Furthermore, collision-avoidance requirements could be added as an additional constraint to the optimization problem.

References

[1] Schaub, H., and Junkins, J. L., *Analytical Mechanics of Space Systems*, AIAA Education Series, AIAA, Reston, VA, 2003, pp. 593–669.

[2] Ulybyshev, Y., "Long-Term Formation Keeping of Satellite Constellation Using Linear-Quadratic Controller," *Journal of Guidance, Control, and Dynamics*, Vol. 21, No. 1, Jan.–Feb. 1998, pp. 109–115. doi:10.2514/2.4204

[3] Rahmani, A., Mesbahi, M., and Hadaegh, F. Y., "On the Optimal Balanced-Energy Formation Flying Maneuvers," *AIAA Guidance, Navigation and Control Exhibit*, San Francisco, AIAA Paper 2005-5836, Aug. 2005.

[4] Inalhan, G., Tillerson, M., and How, J. P., "Relative Dynamics and Control of Spacecraft Formations in Eccentric Orbits," *Journal of Guidance, Control, and Dynamics*, Vol. 25, No. 1, Jan.–Feb. 2002, pp. 48–59. doi:10.2514/2.4874

[5] Schaub, H., Vadali, S. R., Junkins, J. L., and Alfriend, K. T., "Spacecraft Formation Flying Control Using Mean Orbit Elements," *Journal of the Astronautical Sciences*, Vol. 48, No. 1, Jan.–Mar. 2000, pp. 69–87.

[6] de Queiroz, M. S., Kapila, V., and Yan, Q., "Adaptive Nonlinear Control of Multiple Spacecraft Formation Flying," *Journal of Guidance, Control, and Dynamics*, Vol. 23, No. 3, May–June 2000, pp. 385–390. doi:10.2514/2.4549

[7] Schaub, H., and Alfriend, K. T., "Hybrid Cartesian and Orbit Element Feedback Law for Formation Flying Spacecraft," *Journal of Guidance, Control, and Dynamics*, Vol. 25, No. 2, Mar.–Apr. 2002, pp. 387–393. doi:10.2514/2.4893

[8] Carter, T. E., "Optimal Power-Limited Rendezvous for Linearized Equations of Motion," *Journal of Guidance, Control, and Dynamics*, Vol. 17, No. 5, Sept.–Oct. 1994, pp. 1082–1086. doi:10.2514/3.21313

[9] Mishne, D., "Maintaining Periodic Relative Trajectories of Satellite Formation by Using Power-Limited Thrusters," AAS/AIAA Astrodynamics Specialists Conference, Big Sky, MT, American Astronautical Society Paper 03-656, Aug. 2003.

[10] Sharma, R., Sengupta, P., and Vadali, S. R., "Near-Optimal Feedback Rendezvous in Elliptic Orbits Accounting for Nonlinear Differential Gravity," *Journal of Guidance, Control, and Dynamics*, Vol. 30, No. 6, Nov.–Dec. 2007, pp. 1803–1813. doi:10.2514/1.26650

[11] Bryson, A., and Ho, Y.-C., *Applied Optimal Control*, Hemisphere, New York, 1975, pp. 42–79, 177–194.

[12] Slotine, J. E., and Li, W., *Applied Nonlinear Control*, Prentice–Hall, Upper Saddle River, NJ, 1991, pp. 100–107.

[13] Hamel, J., and de Lafontaine, J., "Linearized Dynamics of Formation Flying Spacecraft on a J_2-Perturbed Elliptical Orbit," AAS/AIAA Astrodynamics Specialist Conference, Mackinac Island, MI, American Astronautical Society Paper 07-301, Aug. 2007.

[14] Hamel, J., and de Lafontaine, J., "Linearized Dynamics of Formation Flying Spacecraft on a J_2-Perturbed Elliptical Orbit," *Journal of Guidance, Control, and Dynamics*, Vol. 30, No. 6, Nov.–Dec. 2007, pp. 1649–1658. doi:10.2514/1.29438